Topological Phase Diagram of a Two-Subband Electron System

X. Y. Lee and H. W. Jiang
Department of Physics and Astronomy, University of California at Los Angeles, Los Angeles, California 90095

W. J. Schaff
Department of Electrical Engineering, Cornell University, Ithaca, New York 14853
(Received 10 May 1999)

We present a phase diagram for a two-dimensional electron system with two populated subbands. Using a gated GaAs/AlGaAs single quantum well, we have mapped out the phases of various quantum Hall states in the density-magnetic field plane. The experimental phase diagram shows a very different topology from the conventional Landau fan diagram. We find regions of negative differential Hall resistance which are interpreted as preliminary evidence of the long sought reentrant quantum Hall transitions. We discuss the origins of the anomalous topology and the negative differential Hall resistance in terms of the Landau level and subband mixing.

PACS numbers: 73.40.Hm, 71.30.+h, 72.20.My

Extensive work has been carried out on modulation-doped GaAs/AlGaAs heterostructures containing a two-dimensional electron gas (2DEG) within the framework of quantum Hall effect [1]. In most of these structures, only one subband is populated. Even though studies of heterostructures with two populated electric subbands have a long history [2], the inherent additional intersubband scattering has precluded a two-subband system from being a primary candidate to study various aspects of quantum Hall effect. Most of the investigations carried out thus far, not surprisingly, have focused on scattering [3] while others dealt with population effects [4]. Recently, it has become increasingly apparent that, in one-band systems, disorder-induced Landau level mixing can play a critical role in the evolution of the quantum Hall effect, especially in the regime of vanishing magnetic fields. Landau level mixing and its effects have been the subjects of numerous recent experimental [5–7] and theoretical [8] studies. Similarly, in a two-subband system, crossing of Landau levels of the two different subbands can lead to substantial mixing even in relatively strong magnetic fields. The consequences of Landau level mixing on the topology of the phase boundaries between different quantum Hall states [9] in the two-band system are expected to be surprising and possibly profound.

To explore some of these consequences, we have conducted a systematic magneto-transport study on gated, modulation-doped GaAs/AlGaAs single quantum well samples in which there are two populated subbands. We have constructed a topological phase diagram of the two-band system. We found this phase diagram to be considerably more complex than the conventional Landau fan diagram. One of the spectacular consequences of its unusual topology is that there are multiple reentrant quantum Hall transitions. We have observed negative differential Hall resistance in certain regions of the density-magnetic field plane (the n-B plane). The negative differential Hall resistance, in our opinion, is indicative of the reentrant quantum Hall transition.

The sample used in this study is a symmetrical modulation-doped single quantum well with a width of 250 Å. Two Si δ-doped layers ($n_d = 8 \times 10^{11}$ cm^{-2}) are placed on either side of the well. There is a 200 Å spacer between the δ-doped layer and the well on each side. Heavy doping creates a very dense 2DEG, resulting in the filling of two subbands in the well. As determined from the Hall resistance data and Shubnikov–de Hass oscillations, the total density is $n = 1.21 \times 10^{12}$ cm^{-2}. The higher subband has a density $n_2 = 3.3 \times 10^{11}$ cm^{-2}, while the lower subband has a density of $n_1 = 8.8 \times 10^{11}$ cm^{-2} at $B = 0$. The electron mobility at zero gate voltage is about 8×10^4 cm^2/V-s. The samples are patterned into Hall bars with a 3:1 aspect ratio using standard lithography techniques. An Al gate was evaporated on top so that, by applying a negative gate voltage, the carrier density can be varied continuously. A total of 9 samples with different lengths (varying from 30 μm to 3 mm) were studied systematically. For consistency, we present here the data from only one sample. During the experiment, the sample was thermally connected to the mixing chamber of a dilution refrigerator. Magnetic fields up to 12 T were applied normal to the plane containing the 2DEG. Standard lock-in techniques with an excitation frequency of about 13 Hz and a current of 10 nA were employed to carry out the magnetoresistance measurements.

A typical trace of the diagonal resistivity ρ_{xx} and the Hall resistivity ρ_{xy} as a function of B at a temperature of 70 mK is shown in Fig. 1. The integer numbers in the figure identify each quantum Hall state by its quantized value in the unit of h/e^2 [i.e., $S_{xy} = (h/e^2)/R_{xy}$]. The peaks in ρ_{xx} represent the positions of the delocalized states, and together they mark the phase boundaries between various quantum Hall states. The electronic wave functions corresponding to delocalized states are extended across the

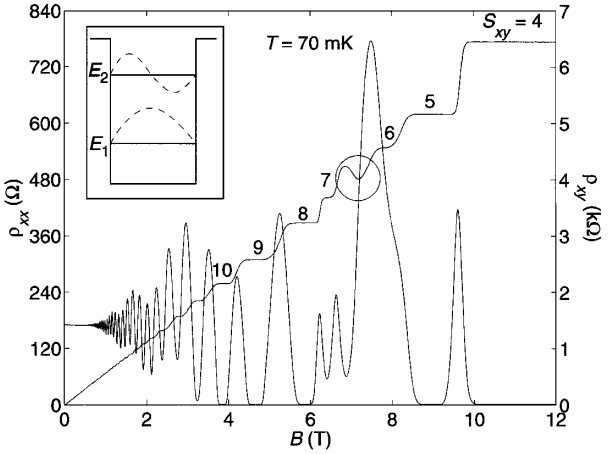

FIG. 1. Longitudinal and Hall resistivity as a function of the magnetic field. Trace was taken at a fixed gate voltage of -0.41 V at $T = 70$ mK. Inset: schematic band diagram of the quantum well with two populated subbands.

system. For the quantum Hall systems, the delocalized states only exist at discrete energy values between two adjacent quantum Hall states [1]. This criterion was used to construct the experimental phase diagram in Fig. 3 below.

Before presenting the experimental phase diagram, it is useful to discuss what one should expect for the simplest case in the absence of Landau level mixing. Using the energy separation between the two subbands for the present sample, we plot in Fig. 2a the energy E as a function of magnetic field. The corresponding positions of the delocalized states in the n-B plane can be calculated, and the resulting phase diagram is displayed in Fig. 2b. From Fig. 2b, one can see that the electrons fill the Landau levels of upper and lower subbands in alternating fashion as the

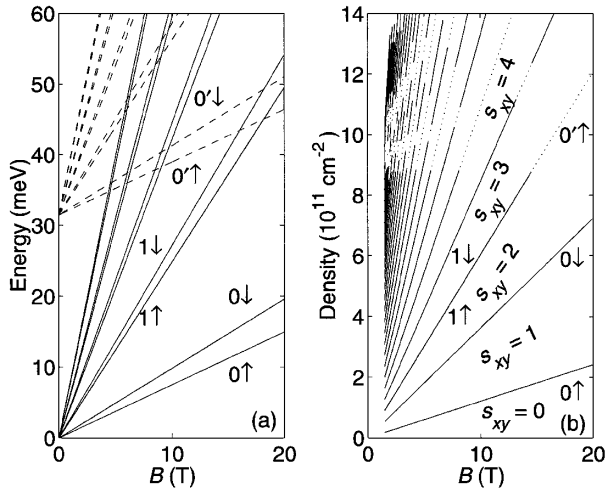

FIG. 2. (a) Energy versus magnetic field for the two-subband system. (b) A map of the delocalized states in the density-magnetic field plane expected for the disorder-free case. The solid lines represent the states populating the first subband and the dashed lines are the ones for the second subband. The numbers indicate the association with the different Landau level indices.

magnetic field is increased. In this case, the phase diagram has an ordinary "fan-like" appearance identical to that for a single-band system.

The actual phase diagram is, however, very different from this simple picture. We present in Fig. 3 an experimental phase diagram. The density on the right axis is related to the gate voltage on the left axis by a linear relation determined by the sample geometry. To construct the phase diagram, we swept both the gate voltage, i.e., the carrier density, at a fixed magnetic field (a "V_g scan") and the field at a fixed gate voltage (a "B scan"). Each peak in ρ_{xx} corresponds to a single data point in the phase diagram. The data points represent the phase boundaries between various quantum Hall liquid states. Limited by the base temperature of our cryostat, the plateaus in regions very near the intersections of phase boundary lines are normally not well resolved. In such cases, we follow the evolutionary development of the plateaus away from these places to assign sensible values of S_{xy}. Moreover, we could not determine the phase boundaries reliably at low magnetic fields ($B \leq 2$ T) as the peaks become progressively more difficult to resolve in a decreasing magnetic field.

In the low-density regime of the phase diagram (i.e., $n \leq 8.5 \times 10^{11}$ cm^{-2}), with the upper subband depopulated, the experimental phase diagram is identical to that of a one-subband system [5]. Note the transition of spin-resolved quantum Hall states to spin-degenerate quantum Hall states at about 8 T. This type of level "pinch off," which is not our primary focus here, has been studied recently in detail experimentally [10]. While the origin of this effect is not completely known, the theoretical model by Folger and Shklovskii suggests that it is a second-order phase transition, much like a ferromagnetic to paramagnetic transition [11]. They argue that the exchange interaction collapses to zero when equal populations of two spin states are reached due to the disorder-induced level broadening. Alternatively, Tikofsky and Kivelson have proposed a different model showing that up- and down-spin electrons in the even-integer filling factors pair together to form the spin-degenerate quantum Hall state [12].

With the upper subband populated, the phase diagram has a very rich topology. The most pronounced feature is the sawtooth-like pattern for densities in the range between $n = 9 \times 10^{11}$ cm^{-2} and 11×10^{11} cm^{-2}. A similar pattern can also be seen for higher densities between $n = 10.5 \times 10^{11}$ cm^{-2} and 12×10^{11} cm^{-2}. There are also apparently "triple" and "quadruple" points which separate the different quantum Hall phases. A triple (quadruple) point is where three (four) boundary lines join together in the phase diagram.

Despite the complexity of this phase diagram, we find that the "selection rules" for the quantum Hall phase transitions are never violated [9]. According to the selection rules, S_{xy} (which simply counts the number of delocalized levels below the Fermi energy) should change by "one" for the spin-resolved case or by "two" for the spin-unresolved case. This can be understood by considering the following.

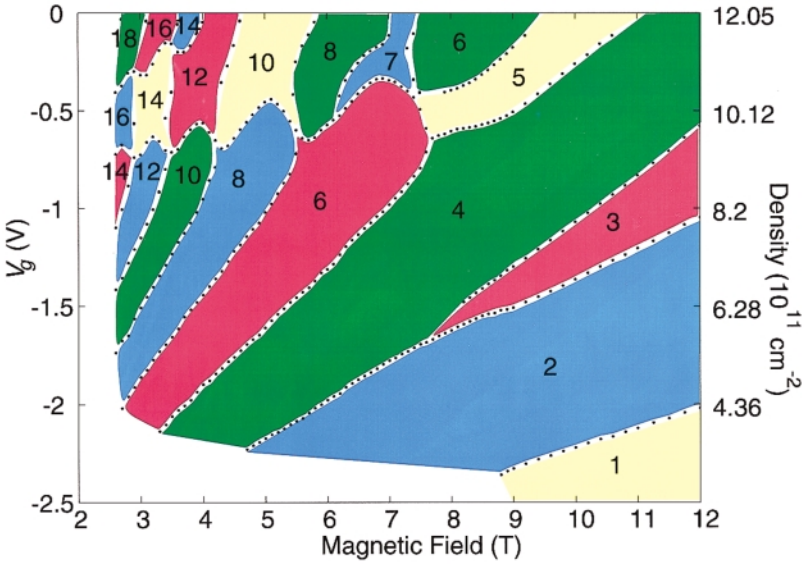

FIG. 3 (color). The experimental phase diagram in the n-B plane. The data points are the phase boundaries. S_{xy} is used to label the various quantum Hall states.

Since the delocalized states exist at discrete energy values (levels), the Fermi level can only cross one delocalized level at a time as the magnetic field or the density is varied, and S_{xy} has to change one by one. As seen in the figure, for either a V_g scan or a B scan, the number for S_{xy} indeed changes either by one for crossing a spin-resolved subband level or by two for crossing a spin-degenerate subband level, or even conceivably by four for crossing a spin-degenerate and subband-mixed level.

One of the striking consequences of this unusual topology is that the differential Hall resistance $d\rho_{xy}/dB$ can be negative (NDHR) during the B scan in certain regions of the n-B diagram. For example a NDHR can be seen in Fig. 1 at about $B = 7$ T (in the circled area). This NDHR is certainly unusual. In a one-band system, only positive differential Hall resistance (i.e., the classical Hall resistance or in the region between two plateaus) and zero differential Hall resistance (i.e., in the plateau region) have been observed. For this two-band system we found, in fact, that NDHR can be seen during a B scan along a trajectory cutting through the top portion of any sawtooth.

We present (shown in the left of Fig. 4) the evolution of the NDHR for various V_g at a fixed temperature of 70 mK for the sawtooth between 6 and 8 T. For the convenience of tracking S_{xy}, we have plotted $1/R_{xy}$ (in units of e^2/h) as the vertical axis so that the values of S_{xy} can be read off directly from the y axis. At $V_g = -0.34$ V (at the tip of the tooth), a slight dip is seen at the middle of the well-developed $h/7e^2$ Hall plateau. As V_g becomes more negative, the dip shows more deviation from $h/7e^2$ and gets progressively deeper and wider. At $V_g = -0.38$ V, the deviation is the greatest while the high-field portion of the $h/7e^2$ plateau is still visible. The high-field side of this dip leads to the unusual NDHR. As the gate voltage gets even more negative, the dip develops into the $h/6e^2$ Hall plateau (see, for example, -0.54 V) giving, eventually, the normal $S_{xy} = 7$ to $S_{xy} = 6$ ("6-7," in short) quantum Hall transition.

We have also investigated the temperature dependence of $d\rho_{xy}/dB$ at $V_g = -0.41$ V. B-scan traces (shown in the right of Fig. 4) were taken at $T = 4.2$ K, 1.2 K, and 70 mK. At the highest temperature, the $h/7e^2$ plateau is not resolved and there was no sign of the NDHR. At $T = 1.2$ K, the plateau starts to form and a small dip becomes visible near the expected positions of the $h/7e^2$ and $h/6e^2$ plateaus. As the temperature goes further down, both $h/7e^2$ and $h/6e^2$ plateaus become well resolved and the dip becomes deeper. The deviation has reached a value of about $h/6.5e^2$ at 70 mK. It is apparent that the NDHR is associated closely with the formation of the quantum Hall states of $S_{xy} = 6$ and $S_{xy} = 7$ in this case.

In an attempt to understand the topological anomalies of the phase diagram, we have performed a simple numerical calculation to account for the effects of the overlap of

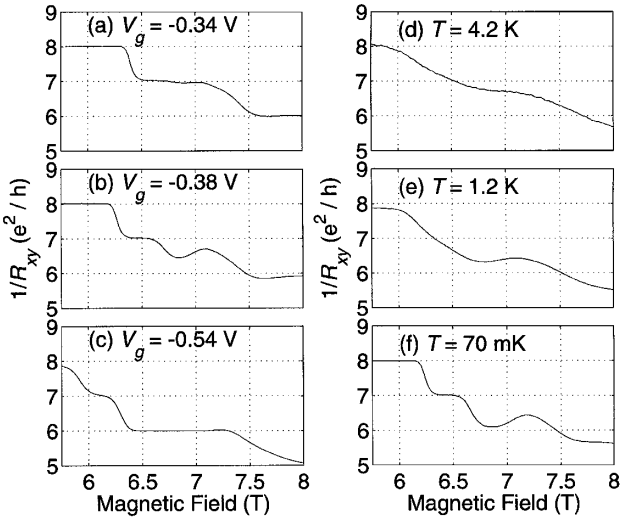

FIG. 4. Left side: $1/R_{xy}$ versus B at three different gate voltages showing the evolution of the negative differential Hall resistance. Right side: $1/R_{xy}$ versus B at $V_g = -0.41$ V at three different temperatures.

Landau levels of two subbands. In this calculation, we have made the simple assumption that the density of states can be modeled as two sequences of Gaussian functions centered around the Landau levels for the lower and upper subbands, respectively. The width of the Gaussian functions is determined from the conductivity of the sample [6]. We then assume that the delocalized states lie at each maximum in the overall density of states, which is the sum of the density of states of the upper and lower subbands. S_{xy} is then simply set equal to the number of delocalized levels below E_F. In this way, we can obtain a theoretical phase diagram. Of course, in reality, the Landau level mixing due to both the level repulsion and the disorder broadening is far more complicated than this simple assumption. Our simple calculation is nevertheless able to produce the sawtooth-like structure qualitatively, as seen in the experimental data. Each time two Landau levels of the two subbands move towards a crossing, the position of the delocalized states (i.e., the maximum in the resultant density of states) deviates from the normal fan lines and "floats up" in density or, equivalently, in energy. At the same time, when the two levels move away from the crossing, the position of the delocalized states "sinks down," back to the normal fan lines. This floating up and sinking down gives rise to the unusual sawtooth patterns. We think this effect has the same origin as the "floating" observed in the one-band system in a vanishing B [5,13]. The sawtooth structure at 7.5 T can be identified as being due to the mixing of the spin-degenerate third Landau level ($N = 2$) of the first subband with the spin-up state of the lowest Landau level of the second subband ($N' = 0\uparrow$). The features at about 5.5, 4.4, and 3.5 T are due to the mixing of the ($N' = 0$) level with ($N = 3, 4, 5$) levels, respectively. Another portion of the sawtooth pattern at high densities is due to the mixing of the ($N' = 1$) level with the $N = 5, 6$ levels.

It is important to point out here that the sawtooth patterns indicate a sequence of reentrant quantum Hall transitions (i.e., 7-6-7, 10-8-10, and 12-10-12, etc.). This type of reentrant quantum Hall transition has been proposed theoretically for single-band quantum Hall systems [9,13]. Experimentally, it has not been seen to date. An analogous transition which has been observed is the reentrant insulator–quantum Hall transition known as the 0-2-0 transition [14] or the 0-1-0 transition [15]. For the present experiment, we believe the NDHR observed in certain regions shows preliminary evidence of the long sought reentrant quantum Hall transitions. For example, in the region between 6 and 8 T, a B scan at the appropriate V_g at the top portion of the sawtooth is equivalent to traversing the phase diagram horizontally, thus cutting through two sides of a sawtooth. To the left of the sawtooth, we can identify the quantum Hall state as $S_{xy} = 7$ state. Inside the sawtooth, it is a $S_{xy} = 6$ state. To the right, within a very narrow range of B, it is again a $S_{xy} = 7$ state. For the 7-6-7 transition, the Hall resistance should vary from $h/7e^2$ to $h/6e^2$ and back to $h/7e^2$ with increasing B. However, the $S_{xy} = 6$ and the "reentrant" $S_{xy} = 7$ plateaus in our experiment cannot be well resolved simultaneously at a given V_g. As a result, the values of the dip and the peak in R_{xy} only reach, at best, about $h/6.5e^2$ rather than $h/6e^2$ and $h/7e^2$, respectively. The NDHR can be considered as a precursor of the reentrant $S_{xy} = 7$ state. We believe one should be able to observe the true 7-6-7 transition at lower temperatures. We, however, cannot eliminate the possibility that a true quantum Hall state (i.e., with zero diagonal resistance and a quantized Hall plateau) would be intrinsically prohibited by the Landau level mixing.

The authors thank S. Kivelson and D. Orgad for helpful discussions. This work is supported by NSF under Grant No. DMR 9705439.

[1] For a review, see *Perspectives in Quantum Hall Effect*, edited by S. Das Sarma and A. Pinzuk (Wiley, New York, 1997).

[2] For an early example, see H. L. Stormer, A. C. Gossard, and W. Wiegmann, Solid State Commun. **41**, 707 (1982).

[3] See, for example, R. Fletcher, E. Zaremba, M. D'Iorio, C. T. Foxon, and J. J. Harris, Phys. Rev. B **41**, 10 649 (1990); R. M. Kusters *et al.*, Phys. Rev. B **46**, 10 207 (1992); V. E. Zhitomirskii, JETP Lett. **55**, 687 (1992).

[4] See, for example, K. Ensslin, D. Heitmann, R. R. Gerhardts, and K. Ploog, Phys. Rev. B **39**, 12 993 (1989); A. R. Hamilton *et al.*, Phys. Rev. B **51**, 17 600 (1995).

[5] I. Glozman, C. E. Johnson, and H. W. Jiang, Phys. Rev. Lett. **74**, 594 (1995).

[6] I. Glozman, C. E. Johnson, and H. W. Jiang, Phys. Rev. B **52**, R14 348 (1995).

[7] S. V. Kravchenko, W. Mason, J. E. Furneaux, and V. M. Podalov, Phys. Rev. Lett. **75**, 910 (1995).

[8] D. Z. Liu and S. Das Sarma, Phys. Rev. B **49**, 2677 (1994); T. V. Shahbazyan and M. E. Raikh, Phys. Rev. Lett. **75**, 304 (1995); V. Kagalovsky, B. Horovitz, and Y. Avishai, Phys. Rev. B **52**, R17 044 (1995); A. Gramada and M. E. Raikh, Phys. Rev. B **54**, 1928 (1996); D. Z. Liu, X. C. Xie, and Q. Niu, Phys. Rev. Lett. **76**, 975 (1996); F. D. M. Haldane and K. Yang, Phys. Rev. Lett. **78**, 298 (1997).

[9] S. Kivelson, D. H. Lee, and S. C. Zhang, Phys. Rev. B **46**, 2223 (1992).

[10] L. W. Wong, H. W. Jiang, and W. J. Schaff, Phys. Rev. B **55**, R7343 (1997).

[11] M. M. Fogler and B. I. Shklovskii, Phys. Rev. B **52**, 17 366 (1995).

[12] A. M. Tikofsky and S. Kivelson, Phys. Rev. B **53**, 13 275 (1996).

[13] The term "floating" was originally introduced by Khmelnitskii and Laughlin [see, D. E. Khmelnitskii, Phys. Lett. **106**, 182 (1984); JETP Lett. **38**, 556 (1983); R. B. Laughlin, Phys. Rev. Lett. **52**, 2304 (1984)]. It has been used widely in the recent literature.

[14] H. W. Jiang, C. E. Johnson, K. L. Wang, and S. T. Hannahs, Phys. Rev. Lett. **71**, 1439 (1993); T. Wang *et al.*, Phys. Rev. Lett. **72**, 709 (1994); R. J. F. Hughes *et al.*, J. Phys. Condens. Matter **6**, 4763 (1994).

[15] D. Shahar, D. C. Tsui, and J. E. Cunningham, Phys. Rev. B **52**, 14 372 (1995).